Cell Death and Differentiation (2012) 19, 1634–1643

www.nature.com/cdd

# MKP-1 antagonizes C/EBP$\beta$ activity and lowers the apoptotic threshold after ischemic injury

A Rininger[1], C Dejesus[1], A Totten[1], A Wayland[2] and MW Halterman*[,1,2,3]

**The dual specificity phosphatase MAPK phosphatase-1 (MKP-1) feeds back on MAP kinase signaling to regulate metabolic, inflammatory and survival responses. MKP-1 is widely expressed in the central nervous system (CNS) and induced after ischemic stress, although its function in these contexts remains unclear. Here we report that MKP-1 activated several cell death factors, including BCL2 and adenovirus E1B 19 kDa interacting protein 3, and caspases 3 and 12 culminating in apoptotic cell death *in vitro*. MKP-1 also exerted inhibitory effects on the bZIP transcription factor CCAAT/enhancer-binding protein (C/EBP$\beta$), previously shown to have neuroprotective properties. These effects included reduced expression of the full-length C/EBP$\beta$ variant and hypo-phosphorylation at the MEK-ERK1/2-sensitive Thr$^{188}$ site. Notably, enforced expression C/EBP$\beta$ rescued cells from MKP-1-induced toxicity. Studies performed in knock-out mice indicate that the MKP-1 activity is required to exclude C/EBP$\beta$ from the nucleus basally, and that MKP-1 antagonizes C/EBP$\beta$ expression after global forebrain ischemia, particularly within the vulnerable CA1 sector of the hippocampus. Overall, MKP-1 appears to lower the cellular apoptotic threshold by inhibiting C/EBP$\beta$ and enhancing both BH3 protein expression and cellular caspase activity. Thus, although manipulation of the MKP-1-C/EBP$\beta$ axis could have therapeutic value in ischemic disorders, our observations using MKP-1 catalytic mutants suggest that approaches geared towards inhibiting MKP-1's phosphatase activity alone may be ineffective.**
*Cell Death and Differentiation* (2012) **19,** 1634–1643; doi:10.1038/cdd.2012.41; published online 20 April 2012

Ischemia is a potent stimulus for *de novo* gene expression, which depending on the duration and severity of the exposure can have opposing effects on cell survival. For example, in transient global ischemia, although mild stress may prime adaptive transcription, severe stress can induce cell death in selectively vulnerable neuronal populations, such as the CA1 field of the hippocampus. Microarray studies implicate a role for both adaptive gene repression and induction of transcripts with toxic potential. Although a range of ischemia-responsive sensor–effector networks have been discovered, far less is known regarding the transitionary mechanisms involved, switching between adaptive and pathological gene expression.[1] A better understanding for these networks and the molecular switches that govern their activity could have therapeutic relevance for disorders in which ischemia is a central component.

One of the transcripts frequently induced in stroke expression array experiments is the non-receptor dual mitogen-activated protein kinase (MAPK) phosphatase-1 (dual-specificity phosphatases (DUSP)1/MKP-1/CL100). MKP-1 is a 367 amino acid residue protein with a predicted molecular mass of 39.3 kDa and dual specificity for removing phosphorylated tyrosine and threonine residues.[2] MKP-1 is localized in the nucleus, causing the inhibition of G1-specific gene transcription and entry into S-phase in fibroblasts among other effects.[3] MKP-1 stability is regulated by the ubiquitin–proteosome pathway, which in turn is inhibited by p42/p44-dependent phosphorylation of its carboxyl terminus.[4] Although MKP-1 can dephosphorylate all three MAPKs, it preferentially inhibits p38 and JNK activity over ERK1/2, providing an important negative feedback loop on a variety of cellular processes, including growth factor signaling, inflammation, differentiation and apoptosis.[5] And despite the potential for redundancy among the large repertoire of cellular phosphatases identified, MKP-1 knock-out (KO) mice exhibit heightened inflammation, autoimmunity and metabolic defects.[6,7] Clues from the literature also suggest MKP-1 activity is associated with cell injury. MKP-1 is a target of the pro-apoptotic transcription factors p53 and E2F-1, and accumulates following oxidant, hyperosmotic or hypoxic stress.[8] MKP-1 may also potentiate neurotoxicity by inhibiting the transcriptional activity of the hypoxia-inducible factor HIF-1$\alpha$, which is a master regulator of neuroprotective genes, including vascular endothelial growth factor and erythropoietin.[9]

Like MKP-1, the bZIP transcription factor C/EBP$\beta$ regulates developmental, metabolic and inflammatory responses *in vivo*.[6,7] In addition to its effects on general transcriptional potency, MEK-dependent phosphorylation of C/EBP$\beta$ at Thr$^{188}$ biases cortical progenitors towards a neuronal fate in

[1]Department of Pediatrics, University of Rochester Medical Center, Rochester, NY, USA; [2]Center for Neural Development and Disease, University of Rochester Medical Center, Rochester, NY, USA and [3]Department of Neurology, University of Rochester Medical Center, Rochester, NY, USA
*Corresponding author: MW Halterman, Center for Neural Development and Disease, University of Rochester Medical Center, 601 Elmwood Avenue, Box 645, 14642, Rochester, NY, USA. Tel: (585) 273-1335; Fax: (585) 276-2739; E-mail: marc_halterman@urmc.rochester.edu
**Keywords:** C/EBP$\beta$; MKP-1; phosphatase; hypoxia; ischemia; neuron
**Abbreviations:** MAPK, mitogen-activated protein kinase; MKP-1, MAPK phosphatase-1; C/EBP$\beta$, CCAAT/enhancer binding protein; IRES, internal ribosomal entry site; PARP, poly (ADP-ribose) polymerase; BNIP3, BCL2 and adenovirus E1B 19 kDa interacting protein 3; NIX, NIP3-like protein X; LAP, liver-enriched activator protein; LIP, liver-enriched inhibitor protein; ER, endoplasmic reticulum
Received 28.9.11; revised 12.3.12; accepted 12.3.12; Edited by RA Knight; published online 20.4.12

the developing CNS.[10,11] Although it is not yet known whether stress-induced MKP-1 antagonizes the pro-survival function of C/EBP$\beta$ in the injured adult nervous system, we found that loss of C/EBP$\beta$ expression in hypoxic neurons promotes cell death *in vitro*,[12] suggesting the stoichiometric relationship between the available pool of bZIP heterodimeric partners particularly important.[12,13] In the present study, we test the hypothesis that MKP-1 serves a molecular switch, exerting similar suppressive effects on the pro-survival factor C/EBP$\beta$ following ischemic injury as has previously been described for HIF-1$\alpha$.[9] Our results indicate that MKP-1 promotes cellular toxicity in part by altering the normal pattern of C/EBP$\beta$ expression, thereby priming classical apoptotic signaling cascades, usually activated after prolonged ischemic stress. Moreover, we show that MKP-1's antagonistic effects on C/EBP$\beta$ occur *in vivo* as well, affecting ischemia-sensitive regions of the adult mouse hippocampus following transient forebrain ischemia. These data suggest that pharmacological agents that inhibit MKP-1-C/EBP$\beta$ signaling could be used to protect against neuronal injury after ischemia, or in related disorders where ischemia is a central component.

## Results

Between 30–40% of dissociated cortical neurons exposed to continuous hypoxia undergo transcription-dependent cell death marked by changes in the expression of Bcl-2 related proteins, the cleavage of cellular caspases, and ultimately, nuclear condensation and pyknosis. To define the early signaling events involved in this pathological response, we used expression microarrays and identified MKP-1 as a candidate modifier transcript expressed transiently within the first three hours of hypoxia.[14] To validate the observed dynamics of the MKP-1 expression, we harvested total RNA and protein from primary cortical cultures and analyzed MKP-1 expression by qPCR and western blotting (Figures 1a and b). Hypoxia transiently stimulated levels of MKP-1 message ($1.0 \pm 0.4$ *versus* $3.9 \pm 2.6$, $P = < 0.01$) and protein in primary neuronal cultures. MKP-1 induction at the protein level was observed within 6 h of exposure preceding activation of cell death markers, including transcriptional induction of the apoptotic factor BCL2 and adenovirus E1B 19 kDa interacting protein 3 (BNIP3; $1.0 \pm 0.5$ *versus* $9.2 \pm 2.9$, $P = < 0.001$) and cleavage of the caspase-3 substrate poly (ADP-ribose) polymerase (PARP; Figure 1b).

To test the hypothesis that MKP-1 expression sensitized cells to delayed injury, we determined whether transfection of a chimeric GFP-MKP-1 fusion would exhibit toxicity in HN33 cultures. Although the inhibitory effects of MKP-1 on MAPK signaling is often ascribed to the catalytic function of the protein tyrosine phosphatase (PTP) domain, MKP-1 also contains two amino-terminal cdc25 homology domains (CH2A and CH2B) capable of perturbing MAPK activity through substrate competition (Figure 2a).[5] We therefore compared the survival effects of GFP-MKP-1 constructs lacking the CH2AB (GFP-$\Delta$AB) or PTP homology domains (GFP-AB) against GFP-MKP-1 or GFP alone. Western blotting of crude lysates indicated that relative to GFP, the GFP-MKP fusions exhibited uniformly lower expression levels (Figure 2b), an effect likely related to ubiquitin-mediated turnover of MKP-1.[4]

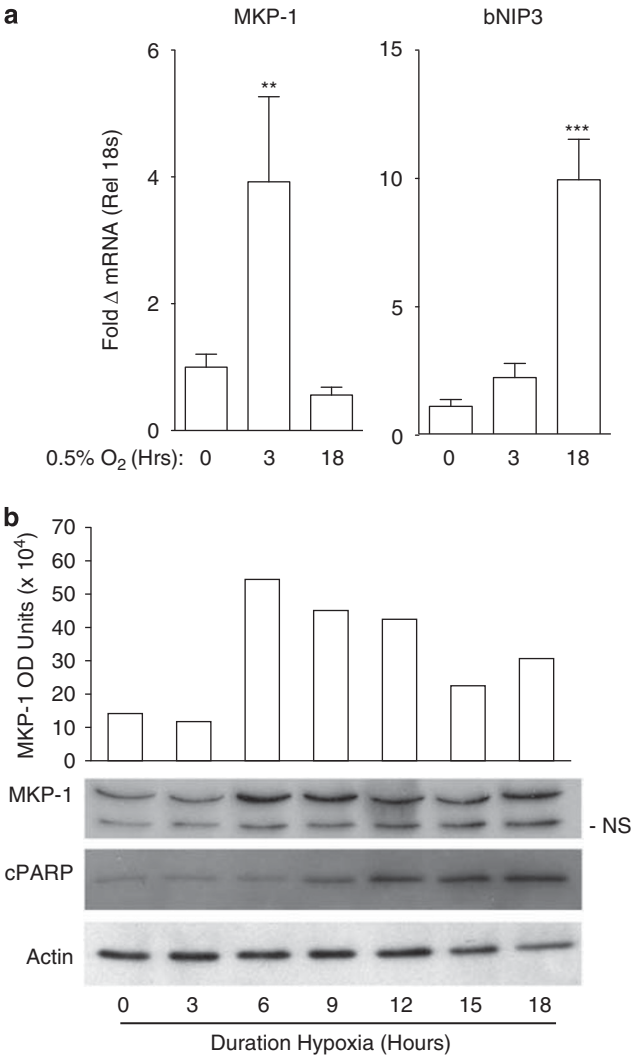


**Figure 1** Hypoxic exposure induces MKP-1 expression in primary neurons and precedes the activation of apoptotic markers. (**a**) cDNA generated from DIV7 embryonic cortical neurons exposed to varying times in hypoxia (0.5% $O_2$) were analyzed by quantitative PCR for MKP-1 and bNIP3 expression. Reactions were performed in triplicate and normalized against endogenous 18S rRNA. Data are shown as the average fold induction ± S.D. relative to normoxic controls ($** = P < 0.01$, $*** = P < 0.001$, $N = 3$). (**b**) Western blotting time-course analysis performed on lysates from DIV7 cortical neuronal cultures exposed to 0.5% $O_2$ for the times indicated. Densitometry indicates that MKP-1 was induced at the protein level within 6 h hours exposure and correlated with the delayed onset of PARP cleavage. Total actin levels are shown to control for loading in the face of hypoxia-induced cell loss

In terms of their effects on survival, expression of all GF-MKP constructs caused a time-dependent increase in nuclear pyknosis not observed with an empty vector or GFP-transfected controls (Figures 2c and d). As predicted, full-length GFP-MKP-1 toxicity manifest within 24h relative to GFP-transfected controls ($38.6 \pm 11.0\%$ *versus* $11.5 \pm 6.1\%$, $P = < 0.05$). After 48h in culture, both the GFP-AB and GFP-$\Delta$AB constructs produced significant injury relative to GFP alone ($50.8 \pm 6.7\%$ and $41.6 \pm 1.7\%$ *versus* $15.94 \pm 3.0\%$, $P = < 0.01$). These data indicate that both the phosphatase and non-catalytic cdc25 homology domains contribute to toxic effects of MKP-1 *in vitro*.

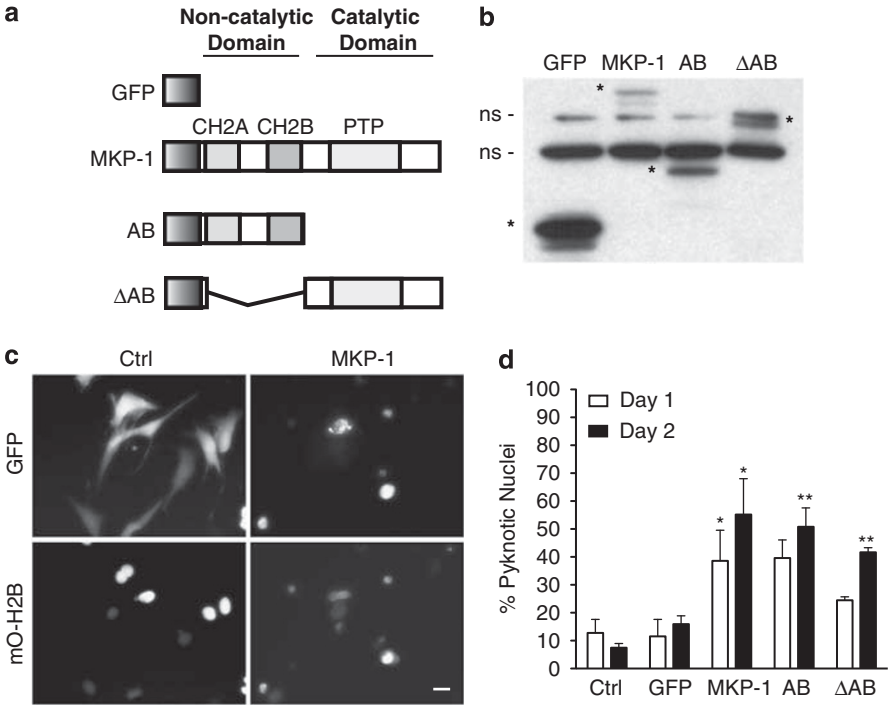


**Figure 2** Expression of MKP-1 is toxic to HN33 cells. (**a**) Schematic of GFP-MKP constructs used in this study. The cdc25 homology domains (CH2A and CH2B) located in the amino-terminal portion of the PTP in the carboxyl terminus located downstream of the GFP open-reading frame are shown. (**b**) Western analysis confirms comparable levels of expression for the GFP-MKP fusions in normoxic HN33 cells. (**c**) GFP-MKP-1 induces nuclear condensation and pyknosis in the HN33 line visualized using the co-transfected mOrange-H2B reporter. (**d**) Nuclear pyknosis counts indicate that full-length and deletion mutant GFP-MKP-1 constructs induce injury in HN33-cultured cells. Data are shown as the fraction of pyknotic nuclei *versus* the total. Test samples are compared with GFP control for significance testing (avg ± S.D.; ** = $P<0.01$, *** = $P<0.001$, $N=3$). Asterisks denote the expected weight of the expressed product detected with GFP antisera

To address the potential off-target effects on non-MKP-1 substrates caused by sustained MKP-1 expression, we next generated tetracycline-inducible stable HN33.11 lines expressing either MKP-1 (MKP-WT-IRES-GFP), the phosphatase-dead mutant MKP-$1^{CS}$ (MKP-$1^{CS}$-IRES-GFP) or GFP alone (MCS-IRES-GFP). Because of the inherent leakiness of the pBIG2i system, low-level transgene expression was seen in the absence of ligand (Figure 3a). Exposure to doxycycline (dox; 1 $\mu$g/ml) produced transgene induction within 6 h in all lines. Although MKP-1 levels plateaued within 12 h, levels of the MKP-$1^{CS}$ mutant increased throughout the experimental time course, suggesting that the cysteine mutation interfered with the kinetics of MKP-1 turnover. On routine passage, we noted that MKP-1 stable cell counts were reduced compared with either control ($1.9\times10^6\pm0.3$ *versus* $3.0\times10^6\pm0.4$, $P=<0.001$) or MKP-$1^{CS}$ ($2.6\times10^6\pm0.5$, $P<0.005$) stables consistent with the inhibitory effects of MKP-1 on cell division.[3] Considering that this difference could reflect cell loss through induced apoptotic signaling, we investigated the effects of MKP-1 on cleaved caspase-3 activity. In the control line, hypoxia stimulated caspase-3 cleavage (Figure 3c, lane 1 *versus* 3; 0.5% $O_2$, 24 h), whereas dox exposure alone conferred partial protection (lane 3 *versus* 4) as previously reported.[15] In contrast, MKP-1 stables exhibited higher levels of caspase-3, further induced by hypoxia (lanes 1 *versus* 5 *versus* 7). MKP-$1^{CS}$ had intermediate effects despite higher levels of expression (lane 1 *versus* 9). Induction of MKP-1 or MKP-$1^{CS}$ did not enhance toxicity further, likely due to protective effects of dox.

Aside from their role as the executioners of cell death, cellular caspases participate in non-apoptotic events including synaptic plasticity and cellular differentiation.[16] To confirm the extent of the toxic effects of MKP-1 in our system, we extended the analysis in dox-naive stables, surveying additional apoptotic signaling intermediates both proximate and distal to caspase-3 cleavage. Interestingly, basal MKP-1 expression in dox-naive stables was sufficient to induce cell death markers under control conditions mimicking the hypoxic phenotype in control cells. MKP-1 and MKP-$1^{CS}$ further stimulated hypoxia-induced cleavage of caspase-3 and PARP within the 4- to 8-h time points (Figure 4). Interestingly, stables expressing the phosphatase-dead MKP-$1^{CS}$ form exhibited higher overall levels of caspase-12 cleavage under hypoxic conditions relative to both control and MKP-1-expressing lines. And compared with GFP-expressing controls, MKP-1 and MKP-$1^{CS}$ enhanced expression of the pro-apoptotic BH3 proteins BNIP3, NOXA and NIP3-like protein X (NIX) (BNIP3L) to varying degrees. These results support the hypothesis that MKP-1 expression promotes a hypoxic signaling milieu even under normoxic conditions, and that both the non-catalytic amino-terminal cdc25 homology domain as well as the catalytic phosphatase domain convey the toxic effects of MKP-1 (Figure 5).

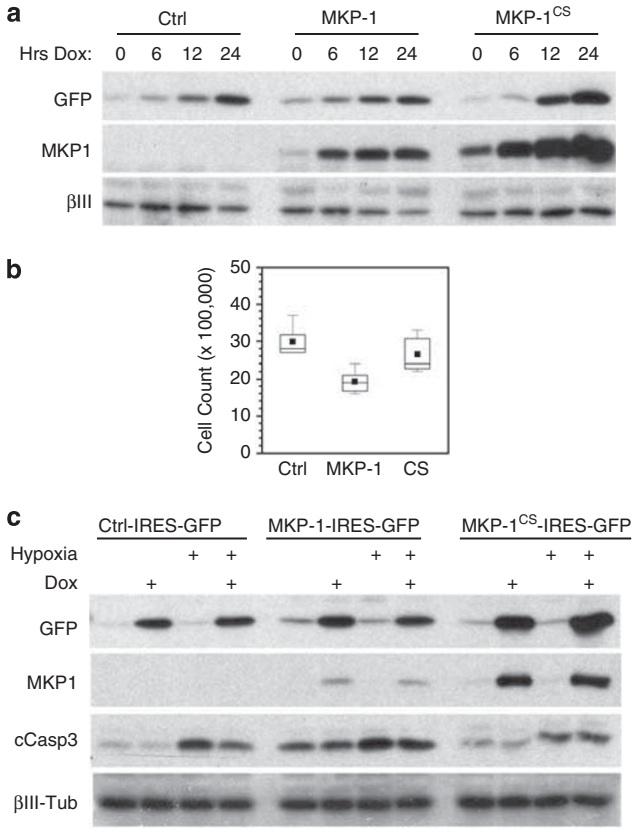


**Figure 3** Characterization of inducible MKP-1 expression in HN33 stable cell lines. (**a**) Western blot analysis of GFP and MKP-1 transgene expression after exposure to dox (1 $\mu$g/ml) in control (MCS-IRES-GFP), WT (MKP-1-IRES-GFP) and phosphatase-deficient (MKP-1$^{CS}$-IRES-GFP) HN33 stables. (**b**) Basal expression of MKP-1 attenuates HN33.11 growth relative to control and CS mutant stables. Cell counts derived from serial passage were performed on each stable line by seeding 300 000 cells in 60-mm dishes and counting viable cells after 3 days in passage. Data are shown as whisker box plots from replicate measures ($N=5$). (**c**) Western blot analysis of cleaved caspase-3 levels in stable lines exposed to dox and hypoxia. Each of three lines were cultured under control conditions, exposed to dox, hypoxia or a combination of both dox and hypoxia before total lysates were harvested and analyzed by western blotting for GFP, MKP-1 and cCasp-3 levels. In both western blots, $\beta$-III tubulin was used to control for equivalent total protein loading

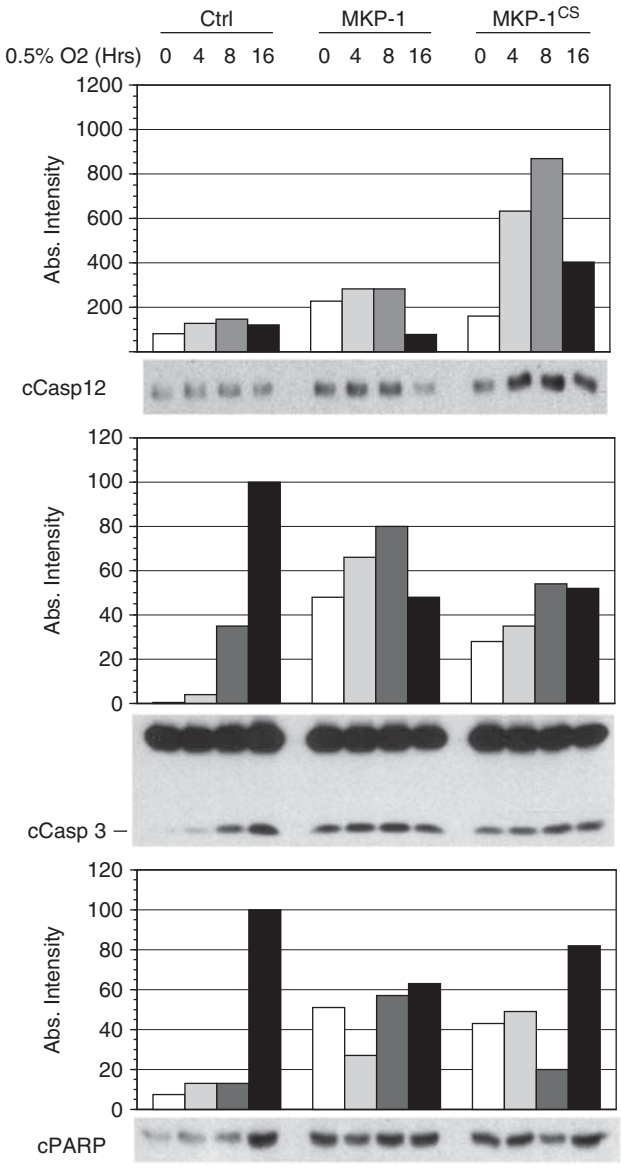


**Figure 4** MKP-1 sensitizes HN33.11 cells to hypoxia-induced apoptosis in hypoxic HN33 lines. Control, MKP-1 and MKP-1$^{CS}$ stable lines were exposed to hypoxia (0.5% $O_2$) for the time periods indicated, and analyzed for the apoptotic markers cCasp3, cCasp12 and cPARP by western blotting. Quantitative analyses were performed using image densitometry with data presented as the absolute intensity

To determine whether stress-induced MKP-1 antagonizes the pro-survival function of C/EBP$\beta$ in the model system, we first investigated what effect the wild type (WT) and phosphatase-dead mutant had on C/EBP$\beta$ protein levels. C/EBP$\beta$ contains several initiator codons that support the translation of both transcriptionally active liver-enriched activator protein ((LAP)1 and LAP2) and dominant-negative liver-enriched inhibitor protein (LIP) C/EBP$\beta$ species.[17] Using time-course analyses, we found that although hypoxia induced the expression of the most transcriptionally active LAP1 form in control lines, both MKP-1 and MKP-1$^{CS}$ markedly inhibited LAP1 expression with lesser suppressive effects on the internally translated species (Figure 6). And although the effects on LAP2 expression were less severe, both MKP-1 and MKP-1$^{CS}$ reduced phosphorylation at the Thr$^{188}$ site required for the full transcriptional activity of C/EBP$\beta$. To link these observed dynamic shifts in the pattern C/EBP$\beta$ isoform expression with MKP-1-induced toxicity, we performed a complementation analysis using C/EBP$\beta$ mutants mutated at the first (C/EBP$\beta\Delta$A) and last (C/EBP$\beta\Delta$C) translation initiation sites. When transfected in HN33 lines, WT C/EBP$\beta$ generated all three major forms, including several smaller products generated through calpain-mediated cleavage (p14, p20 and p20*).[18] In contrast, the $\Delta$A and $\Delta$C point mutants were defective in their expression of LAP1 and LIP, respectively (Figure 7a). As seen before, transfection of GFP-MKP-1 induced nuclear pyknosis in HN33 cells cultured under normoxic conditions (10.0 $\pm$ 3.2% *versus* 40.5 $\pm$ 1.3%, $P<0.001$). However, compared with the cells

receiving MKP-1 alone, cells co-transfected with either WT ($27.9 \pm 4.3\%$ *versus* $40.5 \pm 1.3\%$, $P < 0.05$) or the C/EBP$\beta\Delta$C ($23.4 \pm 1.1\%$ *versus* $40.5 \pm 1.3\%$, $P < 0.01$) exhibited lower levels of nuclear pyknosis (Figures 7b and c). The observation that the LIP-deficient construct provided maximum protection suggests that MKP-1 toxicity involves the disruption of LAP1/2-dependent transcription. We also noted that expression of C/EBP$\beta\Delta$C caused low-level toxicity in GFP-transfected controls ($22.5 \pm 2.8\%$ *versus* $10.0 \pm 3.2\%$, $P < 0.01$), supporting the hypothesis that the ratio of MKP-1 to C/EBP$\beta$ influences net adaptive and pathological transcription under stress conditions.

To test whether MKP-1 exerted suppressive effects on C/EBP$\beta$ activity in the injured adult brain, WT and MKP-1 KO mice were subjected to transient forebrain ischemia. Hippocampal injury was determined by measuring the reduction in nuclear area (i.e., pyknosis and condensation) among CA1 neurons relative to sham controls. Brain sections exhibiting either mild ($80.8 \pm 37\%$ WT and $73.0 \pm 15.2\%$ MKP-1 KO relative to control) or severe ($41.8 \pm 13.8\%$ WT and $32.8 \pm 8.2\%$ MKP-1 KO relative to control) injury were then selected and analyzed for the pattern of C/EBP$\beta$ expression by ICC (Figure 8a). In sham MKP-1 KO mice, overall levels of C/EBP$\beta$ staining were stronger throughout the hippocampus and adjoining brain regions compared with WT controls (Figure 8a, left panels). However, C/EBP$\beta$ expression was reduced in the CA1 field after severe injury, regardless of the MKP-1 status (Figure 8a, right panels). Consistent with the observed *in vitro* effects, MKP KO mice exposed to mild injury exhibited notably higher levels of C/EBP$\beta$ expression in CA1 neurons, compared with injured WT controls. Interestingly, regardless of treatment or genotype, C/EBP$\beta$ signal remained strong within the dentate gyrus, which in terms of neuron survival is relatively ischemia resistant. We also noted that although WT mice exhibited a clear pattern of C/EBP$\beta$ nuclear exclusion within CA1 neurons, C/EBP$\beta$ expression in sham MKP-1 KO mice was both more intense and evenly distributed throughout the nuclear and cytoplasmic compartments (Figure 8b). These data indicate that MKP-1 has distinct effects on C/EBP$\beta$ activity under both basal and stress conditions.

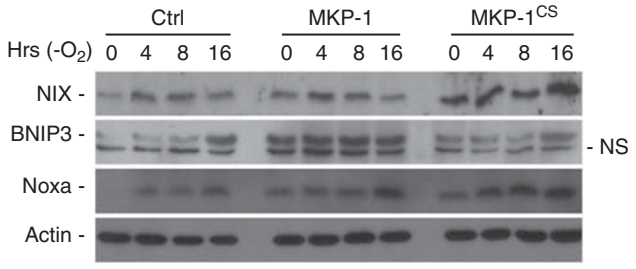


**Figure 5** Effects of MKP-1 expression on basal and hypoxia-inducible expression of several pro-apoptotic BH3 proteins. MKP-1 expression was stimulated by addition of dox (2 $\mu$g/ml) for 12 h before hypoxic (0.5% $O_2$) exposure for the times indicated. Lysates harvested from the HN33.11 stable lines as shown were analyzed by western blotting for BNIP3L (NIX), BNIP3 and NOXA. In these experiments, the predominant form of BNIP3 identified corresponded to the 60-kDa homodimer shown above a faster migrating non-specific band (NS)

## Discussion

MAPK pathways are critical to cellular processes, including cell growth, differentiation and apoptosis. DUSPs feedback on

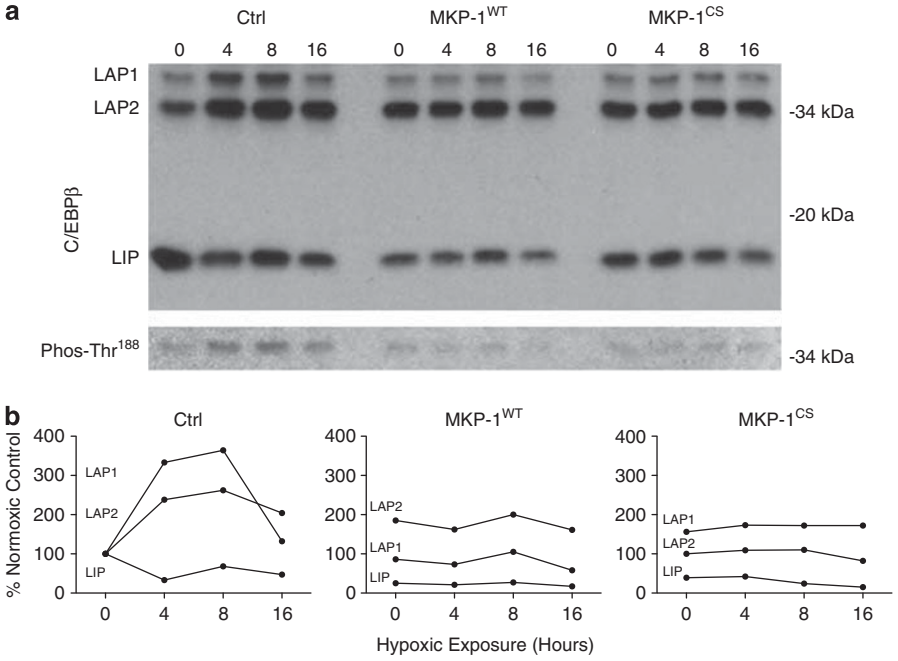


**Figure 6** MKP-1 expression alters the relative expression of the full-length and internally translated forms of the bZIP transcription factor C/EBP$\beta$. (**a**) Dox-naive HN33.11 control, MKP-1$^{WT}$ and MKP-1$^{CS}$ stable lines were exposed to hypoxia (0.5% $O_2$) for the time points shown and analyzed by western blotting using C/EBP$\beta$ antisera. Shown are the expected full-length activator (LAP1), internally translated (LAP2) and inhibitory (LIP) proteins detected in the stable lines. (**b**) Densitometry was performed to quantify the LAP1/LAP2/LIP expression profiles as shown, and data are presented as the fractional change in expression relative to the normoxic control for each C/EBP$\beta$ species

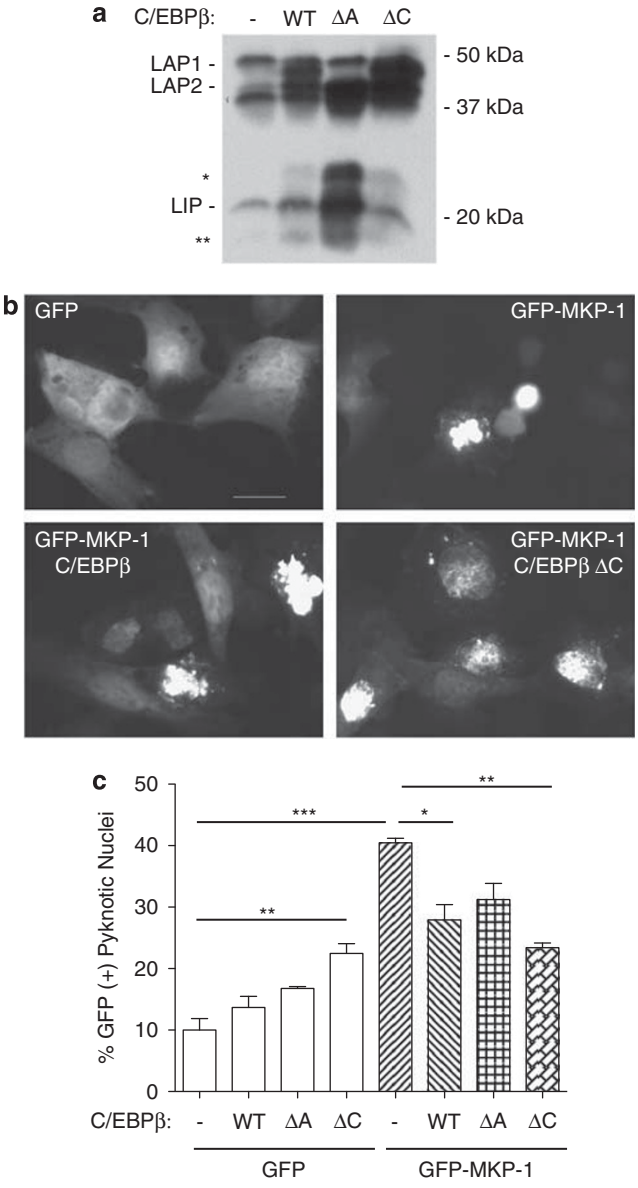


**Figure 7** Transcriptionally active forms of C/EBP$\beta$ rescue HN33.11 cells from MKP-1-mediated toxicity. (**a**) Mutation of the internal methionine initiation codons alters the relative expression levels of the LAP1, and internally translated LAP2 and LIP species of C/EBP$\beta$. Asterisks indicate the smaller 25- and 17-kDa C/EBP$\beta$ forms generated through proteolytic processing. (**b** and **c**) Transfection of MKP-1 induces nuclear pyknosis in recipient cultures, whereas co-transfection of C/EBP$\beta$ and the variant form lacking expression of the LIP inhibitor (C/EBP$\beta\Delta$C) protect against injury. WT HN33.11 cells were seeded to coverslips and transfected either with pWAY21-GFP or pWAY-GFP-MKP-1 (60 ng) and either pSG5 control, WT C/EBP$\beta$, or the LAP1-deficient (C/EBP$\beta\Delta$A) and LIP-deficient (C/EBP$\beta\Delta$C) expression constructs (340 ng). Samples were fixed, Hoechst-stained and analyzed by wide-field fluorescence for nuclear pyknosis (scale bar = 20 $\mu$M). Data are presented as the fraction of pyknotic nuclei relative to pSG5-transfected controls (avg ± S.D. relative to normoxic controls; * = $P<0.05$; ** = $P<0.01$, *** = $P<0.001$, $N=3$)

MAPKs to fine-tune these effects through induced post-translation modification.[2] Despite the potential for functional redundancy among the greater than 100 cellular phosphatases, loss of MKP-1 expression has been linked with specific defects in metabolic, developmental and other fundamental signaling pathways. MKP-1 is broadly expressed in both the developing and adult CNS, and is induced along with other immediate early targets in ischemia-sensitive regions, including the CA1 field of the hippocampus.[1] Although MKP-1 induction could be expected to feedback and limit MAPK-mediated apoptosis effects, we pursued the hypothesis that MKP-1 exerts an overall toxic effect after hypoxia–ischemia. Our results indicate that MKP-1 expression provoked a cascade of events, including the induced expression of several pro-death BH3 proteins, the activation of multiple caspases, and the morphological features of programmed cell death. Moreover, we found that heightened MKP-1 activity antagonized the stability and subcellular distribution of the bZIP factor C/EBP$\beta$ in both cultured cells and in hippocampal CA1 neurons under basal conditions.

MKP-1 expression exhibited consistent effects on the expression of the pro-death BH3 proteins BNIP3 and NOXA, which are activated by ischemia in the cortex and hippocampus, and precede the onset of neuronal death.[19] In the case of BNIP3, beyond potential effects on increasing the rates of transcription, it is possible that MKP-1 may enhance stability or promote the formation of BNIP3 homodimers over the less-toxic monomeric form. Although BNIP3, like Bcl-2 and Bcl-Xl, is a substrate for phosphorylation,[22] it is likely that such an inductive effect would be indirect, as BNIP3 homodimerization requires redox-sensitive interactions between cysteine and histidine residues. In this way, as NOXA and BNIP3 function by neutralizing the cytoprotective effects of Bcl-2 and Bcl-XL,[23] and Bcl-2 enhances cellular antioxidant defenses, higher overall levels of BNIP3 and cellular reactive-oxygen species could also conceivably feed forward to promote BNIP3 dimerization. MKP-1 also accelerated the cleavage of procaspase-9 (data not shown), consistent with reports demonstrating that caspase-9 cleavage is inhibited by MAPK-dependent phosphorylation.[24,25] Given its role as an initiator caspase regulating the cleavage and activation of the executioner caspase-3, this suggests that MAPK–MKP-1–caspase-9 interactions may have a particularly important role in hypoxic neurons. It is also worth commenting on the fact that NOXA, BNIP3 and caspase-12, all localize to the cytosolic side of the endoplasmic reticulum (ER), and that suppression of at least NOXA has been shown to protect against ER stress-induced apoptosis.[20,21] And although we found that MKP-1 also enhanced cleavage of ER stress-associated caspase-12, further analysis will be required to determine whether MKP-1 exhibits particular affinity for modulating ER stress responses.

Our observation regarding the effects of MKP-1 on the CCAAT/enhancer-binding protein C/EBP$\beta$ suggests a proximate cause for MKP-1-induced toxicity. We recently reported that in neurons exposed to chronic hypoxic stress, C/EBP$\beta$ promotes survival by enhancing expression of the pro-survival factor Bcl-2.[12] Given the observed loss of C/EBP$\beta$ LAP1 expression, a plausible mechanism for MKP-1 toxicity could involve the loss of adaptive C/EBP$\beta$-dependent gene expression and subsequent loss of feedback inhibition on p53-dependent pro-apoptotic signaling. In this theoretical model, as MKP-1 is a p53 target, the loss of C/EBP$\beta$-dependent p53 repression would feed forward to further extinguish C/EBP$\beta$ activity. And although the expression of the LAP2 isoform was

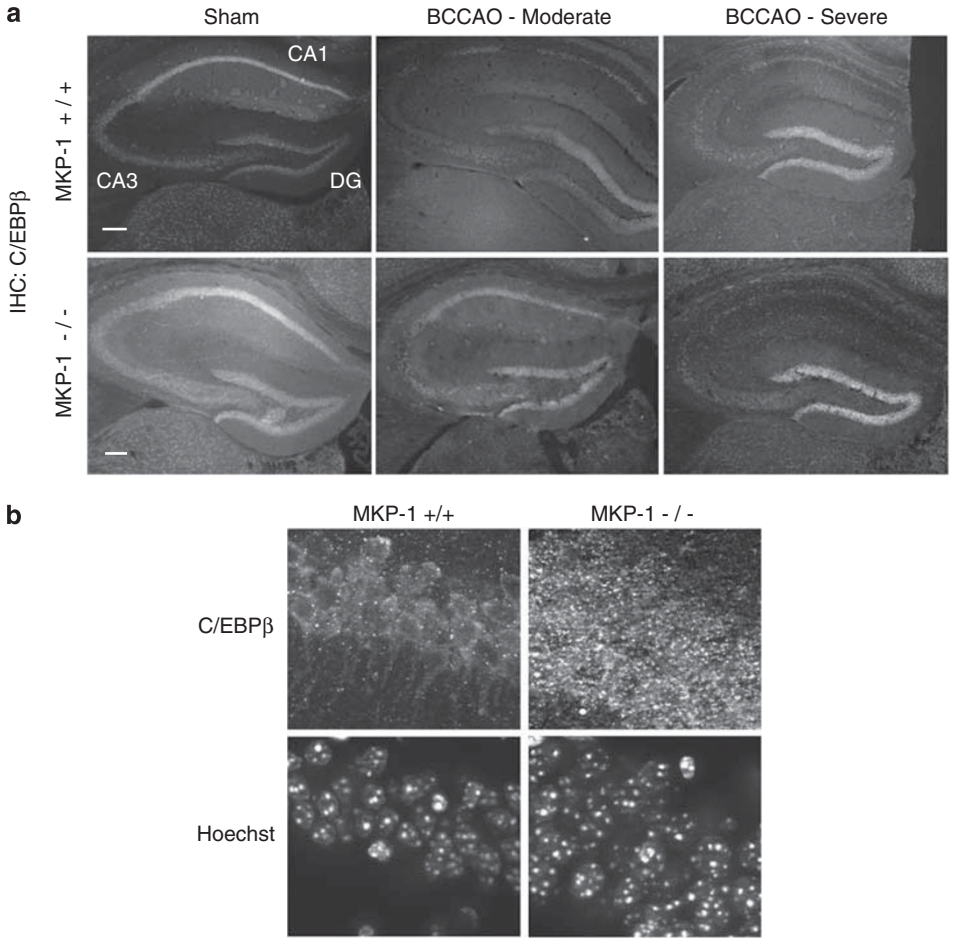


**Figure 8** MKP-1 alters the regional and subcellular pattern of C/EBP$\beta$ expression in the mouse hippocampus. (**a**) WT and MKP-1 KO mice exhibiting either moderate or severe CA1 injury following bilateral carotid artery occlusion were analyzed for C/EBP$\beta$ expression by immunostaining. For orientation, the hippocampal sub-regions of CA1, CA3 and dentate gyrus (DG) are shown. (**b**) Under higher power ( $\times 60$), the pattern of C/EBP$\beta$ expression in WT (MKP-1 $+/+$) CA1 neurons exhibits a predominantly cytoplasmic distribution, whereas the distinction between cytoplasmic and nuclear compartments is lost in MKP-1 $-/-$ samples. Nuclei were visualized using Hoechst (scale bar $= 70\ \mu$M)

increased between 1.6 and 1.8-fold in MKP-1-expressing lines, the fact that LAP2 is less transcriptionally active than the LAP1 form, coupled with the MKP-1 inhibition of Thr$^{188}$ phosphorylation, both compromise the ability of C/EBP$\beta$/LAP2 to support survival in the face of overwhelming stress. Evidence also suggests that loss of C/EBP$\beta$ activity may have a role in ER-dependent cell death signaling. Although it is clearly associated with neuron loss after ischemic injury, expression of the C/EBP$\beta$ heterodimeric partner CHOP-10 alone does not predict neuronal injury *in vitro*.[26,27] Rather, our experience suggests that CHOP-10 acts as a signal amplifier in this system while ischemic susceptibility is determined by the relative stoichiometry between pro-survival (i.e., C/EBP$\beta$) and pro-death (i.e., ATF4) bZIPs.[14] Whether MKP-1 expression exerts analogous effects on the levels and transcriptional activity of CHOP-10, ATF4 or other bZIP, heterodimeric partners activated during the ischemic cascade remains to be seen.

C/EBP$\beta$ belongs to the bZIP family of eukaryotic enhancer-type transcription factors that participate in a wide range of activities, including embryogenesis, metabolism, learning and memory, and ER stress responses.[6,7] The subcellular distribution, stability and transcriptional potency of C/EBP$\beta$ are all MAPK-dependent,[11,28] and hypoxia-dependent changes in MAPK activity can inhibit both C/EBP$\beta$ nuclear translocation and DNA binding.[29] Dimerization between the more than 50 bZIP-containing factors in the human genome governs such activities as nuclear target specificity, subcellular localization and transcriptional potency.[30] Thus, beyond its influence on C/EBP$\beta$ internal translation, the suppressive effect of MKP-1 on overall C/EBP$\beta$ levels likely has wide reaching effects on the broader bZIP signaling network activated during ischemic injury. And aside from the effects on cell survival discussed above, MKP-1-C/EBP$\beta$ interactions appear important in both development and potentially in repair after injury. As previously mentioned, the MEK-dependent phosphorylation at the Thr$^{188}$ site is critical to the pro-neurogenic functions of C/EBP$\beta$.[10,11] C/EBP$\beta$ also stimulates neurite extension through the regulated expression of structural transcripts including $\alpha$-tubulin.[31] In this regard, it was recently demonstrated that MKP-1 has an important role in modulating BDNF-induced axon branching *in vivo*.[32] It will be especially intriguing to determine whether MKP-1-C/EBP$\beta$ interactions influence axonal remodeling and tissue repair after injury.

Although our *in vivo* data clearly indicate that MKP-1 influences C/EBP$\beta$ signaling after global forebrain ischemia, the literature provides a mixed view regarding the influence of MKP-1 on cell survival. Hypoxia and cellular reactive-oxygen species stimulate MKP-1 transcription through the activity of E2F-1 and p53, both of which promote injury after CNS ischemia.[33] In tumor models, MKP-1 activity is associated with tumor survival, chemotherapeutic resistance and with poor long-term patient survival. Likewise, in neural tissue, BDNF–TrkB receptor signaling stimulates MKP-1 activity and facilitates ischemic tolerance, whereas loss of MKP-1 function sensitizes neuronal cells to glutamate-mediated toxicity.[34,35] However, it is possible that like other preconditioning paradigms, low-grade injury induced by MKP-1 produces protection through compensatory induction of endogenous protective genes. It is also possible that MKP-1-C/EBP$\beta$ effects may vary depending on the cellular context. For example, as C/EBP$\beta$ promotes neutrophil activation and heightened inflammation, it is not surprising that C/EBP$\beta$ loss-of-function is neuroprotective after focal stroke.[36] This observation does not however negate the possibility that C/EBP$\beta$ could have entirely different effects on cell autonomous survival and repair of neurons. It is likely that differences in the mechanism of injury, severity of the stimulus and timing will determine which of these opposing activities dominate within ischemia-sensitive structures like the CA1 field of the hippocampus.

In conclusion, we report that the dual specificity phosphatase MKP-1 induces cellular injury through a mechanism involving inhibition of C/EBP$\beta$, induction of pro-death BH3 proteins, and the cleavage of multiple downstream cellular caspases. We also extend these analyses *in vivo* and show that MKP-1 antagonizes the subcellular distribution and stability of C/EBP$\beta$ in CA1 hippocampal neurons global cerebral ischemia. Whether this signaling pathway integrates with either cell-death responses downstream of p53 or the ER stress response remains to be seen. Nonetheless, our findings suggest that strategies geared towards manipulating the MKP-1-C/EBP$\beta$ axis may have particular therapeutic benefit in the CNS ischemia. However, as disruption of the MKP-1 phosphatase activity was insufficient to block cytotoxicity, alternate strategies including those capable of supporting LAP1 expression and C/EBP$\beta$-dependent transcription may prove useful.

## Materials and Methods

**Reagents.** Hoechst 33342, polyethelenimine (PEI), sodium borate, protease inhibitor cocktail (P1754), DMSO and L-glutamine were purchased from Sigma-Aldrich (St Louis, MO, USA). Glutamic acid was purchased from RBI, Inc. (Natick, MA, USA). Cell culture grade 0.25% trypsin–EDTA, Neurobasal media and B27 (antioxidant-plus) supplement were purchased from Invitrogen (Carlsbad, CA, USA). Fetal bovine serum was obtained from Innovative Research (Novi, MI, USA). Transfections were performed using Lipofectamine 2000 according to the manufacturer's instructions (Invitrogen).

**Acute transfection toxicity paradigm.** HN33 cells were generated by crossing mouse hippocampal neurons with the immortalized N18TG2 line as described and passaged in DMEM/HG/8% stripped serum.[37] These cells maintain properties of post-mitotic neurons, including membrane excitability, and have been used previously to study neuronal responses to hypoxic stress. MKP-1-induced toxicity was performed by seeding $4 \times 10^4$ cells to 12-mm glass coverslips and transfecting with either control plasmid (pWay21 or pSG5), the nuclear chromatin reporter mOrange-H2B [38] or constructs expressing forms of MKP or variants of the bZIP factor C/EBP$\beta$. Total amounts of DNA and lipid were kept at a ratio of 400 ng to 1 $\mu$l of Lipofectamine 2000. Cytotoxicity was assessed by counting the degree of nuclear pyknosis from six non-overlapping fields. Slides were blinded before image acquisition and analysis.

**Generation of the HN33.11 stable cell lines and cell growth assays.** The GFP-MKP-1 fusion plasmids pWay21-MKP, pWay-MKP-CH2AB and pWay21-MKP-$\Delta$CH2AB were provided by Dr Anton Bennett (Yale University, New Haven, CT, USA). The cDNAs encoding a C-terminal myc-tagged version of WT human MKP-1 and a catalytically inactive serine-to-cysteine mutation ($Cys^{258}$->Ser) were provided by Nickolas Tonks (CSH, Laurel Hollow, NY, USA).[39] The dox-inducible pBig2i-IRES-GFP construct was generated by sub-cloning the IRES-GFP cassette from pIRES2-GFP (Clontech, Mountain View, CA, USA) into pBIG2i.[40] Likewise, pBIG2i-MKP-1-IRES-GFP and pBIG2i$^{CS}$-IRES-GFP were generated by subcloning myc-MKP-1 cassettes from pSG5-MKP-1-myc and pSG5-MKP-$1^{CS}$-myc into pBIG2i-IRES-GFP. Three HN33 stable lines were then generated by transfection using Lipofectamine 2000 (Invitrogen), followed by selection with hygromycin (600 $\mu$g/ml) for 10 days. After passage in stripped serum, dox-naive stable mixed clones were subjected to FACS to remove subclones constitutively expressing the transgene. For routine passage, cells were maintained in DMEM/HG/8% stripped serum with hygromycin (200 $\mu$g/ml) without dox. For cell growth assays, 300,000 cells were plated to 60-mm well plates and grown in 10% stripped serum in the absence of dox while under selection pressure (200 $\mu$g/ml hygromycin) and standard growth conditions. Data on individual plates prepared serially ($n=5$) for each stable line, trypsinized 3 days after plating, were counted using a stage hemocytometer.

**Primary neuronal cultures.** Culture surfaces were pretreated overnight with filter-sterilized PEI diluted 1 : 500 in sodium borate buffer (150 mM; pH 8.0) and washed three times with sterile $ddH_20$ before use. All protocols were approved by the University of Rochester Committee on Animal Resources (UCAR) and complied with all relevant Federal guidelines. Cortical neuronal cultures were established from timed pregnant WT E15.5 mice using the Neurobasal/B27 media formulation. Briefly, cortical hemispheres were dissected free of meninges, transferred to chilled Dulbecco's phosphate-buffered saline (DPBS; $Ca^{2+}$/$Mg^{2+}$-free) and incubated in 0.25% trypsin (1 ml per hemisphere) for 15 min at room temperature. Trypsin was removed by rinsing three times with MEM, and the tissue was triturated in plating media (Neurobasal media, B27 supplement, 25 mM glutamic acid, 100 mM glutamate) and seeded to 60-mm tissue culture plates (Corning Costar, Corning, NY, USA) at a density of $2.5 \times 10^6$ cells per well.

**Quantitative RT-PCR.** Array expression data were validated by quantitative PCR using an ABI-7700 thermocycler (Applied Biosystems Inc., Foster City, CA, USA). Total RNA was harvested from hypoxic cultures using the RNAeasy Mini Kit (Invitrogen) after hypoxic exposure (0.5%). One milligram of total RNA was reverse transcribed using the High-Capacity cDNA Synthesis Kit (Life Technologies, Grand Island, NY, USA, Cat number 4368814). To determine absolute MKP-1 induction, a standard curve generated using pSG5 and pSG5–MKP-1–Myc. Relative fold induction was determined for bNIP3 by using serial dilution of the normoxic sample (1 : 10 – 1 : 10 000) for the standard curve. Input cDNA (2 $\mu$) was used in 20-$\mu$l reactions using MKP-1 (Cat number Mm00457274), bNIP3 (Cat number Mm01275601) and s18 rRNA (Cat number 4319413E) primer–probe sets (ABI). Reactions were performed in triplicate using Amplitaq Gold master mix (1 cycle $\times$ 55 °C/2 min, 1 cycle $\times$ 95 °C/10 min, 40 cycles $\times$ 95 °C/15 s then 60 °C/1 min). Reactions lacking either template or reverse transcriptase were also run to exclude plasmid and genomic DNA contamination, respectively. Fold-induction calculations for bNIP3 message were made using the comparative $2^{-\Delta\Delta CT}$ method. Values represent the average $\pm$ S.D. across replicates ($n=6$).

**Western blotting and densitometry.** Cell lysates were obtained by rinsing monolayers with ice-cold PBS $\times$ 1 followed by the addition of RIPA buffer containing both protease and phosphatase inhibitor cocktails (Sigma-Aldrich). Samples were boiled in Laemmeli buffer and electrophoresed under reducing conditions on polyacrylamide gels. Proteins were transferred to PVDF membranes and blocked in TBS-T (50 nM Tris-HCl, pH 8.0, 0.9% NaCl and 0.1% Tween-20) containing 5% non-fat dry milk for 1 h at room temperature. Antibodies used in this study included the following: anti-$\beta$-actin (A1978, 1 : 20 000, Sigma), $\beta$ – III tubulin (1 : 500, Sigma), anti-c/EBP$\beta$ (C-19, 1 : 250; Santa Cruz Biotechnology,

Santa Cruz, CA, USA) and MKP-1 (V15, sc1199, Santa Cruz Biologicals, San Diego, CA, USA; 1 : 500). Total caspase 3 (CST9665), cleaved caspase-12 (CST2202), phospho-C/EBP$\beta$-recognizing Thr$^{188}$ in mouse (CST3084) and cleaved PARP (CST9548) were obtained from Cell Signaling Technologies (Danvers, MA, USA). Blots were exposed to HRP-conjugated secondary antibodies (1 : 2000–1 : 5000, Santa Cruz Biologicals) before visualization by ECL chemiluminescence (Pierce, Thermo-Scientific, Rockford, IL, USA).

**Transgenic mice, genotyping protocols and the bilateral Carotid Occlusion Model.** All procedures were approved by the University of Rochester UCAR. MKP-1 KO mice were provided by Anton Bennett (Yale University) with permission from Bristol Myers Squibb (Hopewell, NJ, USA). Tandem PCR analyses were performed for genotyping using AmpliTaq Gold polymerase and primers against MKP-1 (IN5F Fwd: 5′-CTGACAGTGCA GAATCCGGA-3′/ EX1R Rev: 5′-CTATGAAGTCAATAGCCTCGTTGA-3′) and the Neo cassette (1FW005: 5′-ACTGTGTCGGTGGTGCTAATGAGA-3′/1RV006: 5′-TACCGGTGGATGTGGAATGTGT-3′). PCR products were resolved on 1.5% agarose gels. Bands sizes for MKP-1 and the Neo sequences were 650 and 300 bp, respectively. To perform the bilateral carotid occlusion experiments, 8-week-old male WT and MKP-1 KO C57BL/6 mice were anesthetized by i.p. injection of ketamine (100 mg/kg) plus xylazine (10 mg/kg). A midline, ventral neck incision was made, bisecting the maxillary glands. Common carotid arteries (CCAs) were isolated from the vagus nerves, and 6-0 braided silk sutures were used to isolate the arteries from the carotid bundle. S&T vascular clamps ($\sim$50 g/mm$^2$; Fine Science Tools, Foster City, CA, USA) were applied to both CCAs for 10 min. Cessation of blood flow and reperfusion were visually confirmed by direct visualization using a stereomicroscope. After surgery, 500 $\mu$l of warm saline was administered by i.p. injection to aid with recovery. A reflexive heating pad was used to maintain a core temperature of 37 °C during the procedure, and mice were housed at 37 °C in environmental chambers until fully recovered from anesthesia. Sham mice were subjected to all procedures with the exception of clip application. Three days after BCCAO, mice were killed by pentobarbital overdose (150 mg/kg, i.p.) and perfused with 40 ml of ice-cold heparinized saline (10 U/$\mu$L), followed by 40 ml cold 4% PFA in 0.01 M PBS by cardiac puncture. Brains were extracted and post-fixed in 4% PFA overnight at 4 °C, and sunk overnight in 20 and 30% sucrose before sectioning. Each brain was divided into hemispheres, mounted in dry ice, cut into 25 $\mu$m coronal sections on a sliding microtome, and stored at $-$20 °C in cryoprotectant (30% ethylene glycol, 30% sucrose).

Hippocampal sections were mounted on Superfrost slides, allowed to air dry for 1 h, rehydrated for 15 min in PBS and placed into blocking solution (10% goat serum, 1% BSA, 0.5% Triton X-100, 0.05% Tween 20; 2 h, room temperature). Sections were incubated with rabbit anti-C/EBP$\beta$ antisera (Santa Cruz, sc-150, 1 : 300) and incubated at 4 °C overnight. After a single PBS wash, slides were incubated in AlexaFluor 568 nm conjugated goat anti-rabbit antibody for 1 h (1 : 1000, room temperature) and washed three times in PBS. After applying Hoechst 33342 counterstain (10 $\mu$g/ml), slides were mounted using anti-fade media and stored at $-$20 °C until imaged.

**Image analysis and image-based assays.** For nuclear volumetric analyses, *Z*-stack images of two non-overlapping regions within the CA1 field of the hippocampus were acquired using Bitplane (Imaris, South Windsor, CT, USA). Image stacks were condensed to a single flat image through Z Project using Fiji (http://pacific.mpi-cbg.de/wiki/index.php/Fiji). For each image, the outer edges of between 100–120 nuclei were traced using a pen-based graphic tablet (Wacom, Inc., Vancouver, WA, USA). Surface area was calculated for each outlined nucleus within Fiji Analysis. Data from tandem ipsilateral CA1 fields were combined. To determine significance of the BCCAO treatment effect, the average area and S.D. of each sample was calculated in Microsoft Excel. Representative sham, mild and severe injury hemispheres were selected for further IHC and statistical analysis. Data sets were normalized in GraphPad Prism based on their respective sham samples, with the parameter of 100% being set at the average surface area to determine percentage of control nuclear size. Using a linear binning strategy in Microsoft Excel with the CountIF formula application, the normalized nuclear surface areas were distributed into appropriate ranges. In GraphPad Prism, XY Spike Plots of the distribution of nuclear size percent of control were created. For semi-quantitative C/EBP$\beta$ immunohistochemical analyses, all sections were processed for staining in parallel under identical conditions. The image acquisition settings on the microscope and camera were set based on the signal intensity of the brightest sample (sham, MKP-1 KO), and held constant while imaging was performed across other comparison groups.

**Statistical analyses.** Unless otherwise specified, significance testing was performed using either Student's *t*-testing or ANOVA with Newman–Keuls multiple comparison test for *post-hoc* analyses. Results were considered significant for *P*-values $< 0.05$.

## Conflict of Interest

The authors declare no conflict of interest.

**Acknowledgements**. We thank Drs David Rempe, Esta Sterneck, Nina Schor and Anton Bennett for their helpful comments and critical review of the manuscript, and Rita Giuliano for establishing and characterizing the inducible HN33 stable lines. Studies using MKP-1 KO mice were performed with permission from Bristol Myer Squibb (Hopewell, NJ, USA). We thank Dr Calkoven (Leibniz Institute for Age Research, Jena, Germany) for providing the C/EBP$\beta$ internal translation mutants. These studies were supported by grants from the National Institute of Neurological Disease and Stroke to MWH (R00-NS060764).

1. Jin K, Mao XO, Eshoo MW, Nagayama T, Minami M, Simon RP *et al.* Microarray analysis of hippocampal gene expression in global cerebral ischemia. *Ann Neurol* 2001; **50**: 93–103.
2. Keyse SM. Dual-specificity MAP kinase phosphatases (MKPs) and cancer. *Cancer Metastasis Rev* 2008; **27**: 253–261.
3. Brondello JM, McKenzie FR, Sun H, Tonks NK, Pouyssegur J. Constitutive MAP kinase phosphatase (MKP-1) expression blocks G1 specific gene transcription and S-phase entry in fibroblasts. *Oncogene* 1995; **10**: 1895–1904.
4. Brondello JM, Pouysségur J, McKenzie FR. Reduced MAP kinase phosphatase-1 degradation after p42/p44MAPK-dependent phosphorylation. *Science* 1999; **286**: 2514–2517.
5. Wu JJ, Bennett AM. Essential role for mitogen-activated protein (MAP) kinase phosphatase-1 in stress-responsive MAP kinase and cell survival signaling. *J Biol Chem* 2005; **280**: 16461–16466.
6. Bennett AM, Tonks NK. Regulation of distinct stages of skeletal muscle differentiation by mitogen-activated protein kinases. *Science* 1997; **278**: 1288–1291.
7. Liu Y, Shepherd EG, Nelin LD. MAPK phosphatases–regulating the immune response. *Nat Rev Immunol* 2007; **7**: 202–212.
8. Li M, Zhou JY, Ge Y, Matherly LH, Wu GS. The phosphatase MKP1 is a transcriptional target of p53 involved in cell cycle regulation. *J Biol Chem* 2003; **278**: 41059–41068.
9. Liu C, Shi Y, Han Z, Pan Y, Liu N, Han S *et al.* Suppression of the dual-specificity phosphatase MKP-1 enhances HIF-1 trans-activation and increases expression of EPO. *Biochem Biophys Res Commun* 2003; **312**: 780–786.
10. Menard C, Hein P, Paquin A, Savelson A, Yang XM, Lederfein D *et al.* An essential role for a MEK-C/EBP pathway during growth factor-regulated cortical neurogenesis. *Neuron* 2002; **36**: 597–610.
11. Paquin A, Barnabe-Heider F, Kageyama R, Miller FD. CCAAT/enhancer-binding protein phosphorylation biases cortical precursors to generate neurons rather than astrocytes *in vivo*. *J Neurosci* 2005; **25**: 10747–10758.
12. Halterman MW, De Jesus C, Rempe DA, Schor NF, Federoff HJ. Loss of c/EBP-beta activity promotes the adaptive to apoptotic switch in hypoxic cortical neurons. *Mol Cell Neurosci* 2008; **38**: 125–137.
13. Lange PS, Chavez JC, Pinto JT, Coppola G, Sun CW, Townes TM *et al.* ATF4 is an oxidative stress-inducible, prodeath transcription factor in neurons *in vitro* and *in vivo*. *J Exp Med* 2008; **205**: 1227–1242.
14. Halterman MW, Gill M, DeJesus C, Ogihara M, Schor NF, Federoff HJ. The endoplasmic reticulum stress response factor CHOP-10 protects against hypoxia-induced neuronal death. *J Biol Chem* 2010; **285**: 21329–21340.
15. Halterman MW. An improved method for the study of apoptosis-related genes using the tet-on system. *J Biomol Screen* 2011; **16**: 332–337.
16. D'Amelio M, Cavallucci V, Cecconi F. Neuronal caspase-3 signaling: not only cell death. *Cell Death Differ* 2010; **17**: 1104–1114.
17. Calkhoven CF, Muller C, Leutz A. Translational control of C/EBPalpha and C/EBPbeta isoform expression. *Genes Dev* 2000; **14**: 1920–1932.
18. Baer M, Johnson PF. Generation of truncated C/EBPbeta isoforms by *in vitro* proteolysis. *J Biol Chem* 2000; **275**: 26582–26590.
19. Althaus J, Bernaudin M, Petit E, Toutain J, Touzani O, Rami A. Expression of the gene encoding the pro-apoptotic BNIP3 protein and stimulation of hypoxia-inducible factor-1$\alpha$ (HIF-1$\alpha$) protein following focal cerebral ischemia in rats. *Neurochem Int* 2006; **48**: 687–695.
20. Futami T, Miyagishi M, Taira K. Identification of a network involved in thapsigargin-induced apoptosis using a library of small interfering RNA expression vectors. *J Biol Chem* 2005; **280**: 826–831.
21. Zhang L, Li L, Liu H, Borowitz JL, Isom GE. BNIP3 mediates cell death by different pathways following localization to endoplasmic reticulum and mitochondrion. *Faseb J* 2009; **23**: 3405–3414.

22. Kubli DA, Quinsay MN, Huang C, Lee Y, Gustafsson AB. Bnip3 functions as a mitochondrial sensor of oxidative stress during myocardial ischemia and reperfusion. *Am J Physiol Heart Circ Physiol* 2008; **295**: H2025–H2031.
23. Kelekar A, Thompson CB. Bcl-2-family proteins: the role of the BH3 domain in apoptosis. *Trends Cell Biol* 1998; **8**: 324–330.
24. Fujita E, Kouroku Y, Jimbo A, Isoai A, Maruyama K, Momoi T. Caspase-12 processing and fragment translocation into nuclei of tunicamycin-treated cells. *Cell Death Differ* 2002; **9**: 1108–1114.
25. Allan LA, Morrice N, Brady S, Magee G, Pathak S, Clarke PR. Inhibition of caspase-9 through phosphorylation at Thr 125 by ERK MAPK. *Nat Cell Biol* 2003; **5**: 647–654.
26. DeGracia DJ, Montie HL. Cerebral ischemia and the unfolded protein response. *J Neurochem* 2004; **91**: 1–8.
27. Osada N, Kosuge Y, Ishige K, Ito Y. Characterization of neuronal and astroglial responses to ER stress in the hippocampal CA1 area in mice following transient forebrain ischemia. *Neurochem Int* 2010; **57**: 1–7.
28. Piwien Pilipuk G, Galigniana MD, Schwartz J. Subnuclear localization of C/EBP beta is regulated by growth hormone and dependent on MAPK. *J Biol Chem* 2003; **278**: 35668–35677.
29. Park YK, Park H. Prevention of CCAAT/enhancer-binding protein beta DNA binding by hypoxia during adipogenesis. *J Biol Chem* 2010; **285**: 3289–3299.
30. Deppmann CD, Alvania RS, Taparowsky EJ. Cross-species annotation of basic leucine zipper factor interactions: Insight into the evolution of closed interaction networks. *Mol Biol Evol* 2006; **23**: 1480–1492.
31. Nadeau S, Hein P, Fernandes K, Peterson A, Miller F. A transcriptional role for C/EBP $\beta$ in the neuronal response to axonal injury. *Mol Cell Neurosci* 2005; **29**: 525–535.
32. Jeanneteau F, Deinhardt K, Miyoshi G, Bennett AM, Chao MV. The MAP kinase phosphatase MKP-1 regulates BDNF-induced axon branching. *Nat Neurosci* 2010; **13**: 1373–1379.
33. Yang H, Wu GS. p53 Transactivates the phosphatase MKP1 through both intronic and exonic p53 responsive elements. *Cancer Biol Ther* 2004; **3**: 1277–1282.
34. Choi BH, Hur EM, Lee JH, Jun DJ, Kim KT. Protein kinase Cdelta-mediated proteasomal degradation of MAP kinase phosphatase-1 contributes to glutamate-induced neuronal cell death. *J Cell Sci* 2006; **119**: 1329–1340.
35. Kim GS, Choi YK, Song SS, Kim WK, Han BH. MKP-1 contributes to oxidative stress-induced apoptosis via inactivation of ERK1/2 in SH-SY5Y cells. *Biochem Biophys Res Commun* 2005; **338**: 1732–1738.
36. Kapadia R, Tureyen K, Bowen KK, Kalluri H, Johnson PF, Vemuganti R. Decreased brain damage and curtailed inflammation in transcription factor CCAAT/enhancer binding protein beta knockout mice following transient focal cerebral ischemia. *J Neurochem* 2006; **98**: 1718–1731.
37. Lee HJ, Hammond DN, Large TH, Wainer BH. Immortalized young adult neurons from the septal region: generation and characterization. *Brain Res Dev Brain Res* 1990; **52**: 219–228.
38. Kremers GJ, Hazelwood KL, Murphy CS, Davidson MW. Piston DW. Photoconversion in orange and red fluorescent proteins. *Nat Methods* 2009; **6**: 355–358.
39. Sun H, Charles CH, Lau LF, Tonks NK. MKP-1 (3CH134), an immediate early gene product, is a dual specificity phosphatase that dephosphorylates MAP kinase *in vivo*. *Cell* 1993; **75**: 487–493.
40. Strathdee CA, McLeod MR, Hall JR. Efficient control of tetracycline-responsive gene expression from an autoregulated bi-directional expression vector. *Gene* 1999; **229**: 21–29.